Effects of IQB-9302 and its enantiomers on a human cardiac potassium channel (Kv1.5)

Investigador Responsable: **Carmen Valenzuela**

(Firma)

Miembros del Equipo Investigador: **Teresa González**

(Firma)

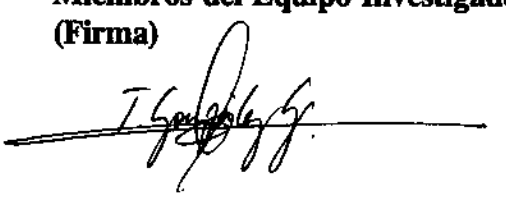

Mónica Longobardo

(Firma)

LOCATION OF THE STUDY: Institute of Pharmacology and Toxicology, CSIC/UCM
School of Medicine. Universidad Complutense
28040 Madrid, SPAIN
Tel. 34-91-394-1474
Fax. 34-91-394-1470
E-mail: carmenva@eucmax.sim.ucm.es

Date of study: November, 22nd, 1999

Introduction

Local anesthetics block the generation and conduction of nerve impulses by inhibiting the current through voltage-gated Na^+ channels in the nerve cell membrane (Hille, 1977; Hondeghem and Katzung, 1977; Strichartz and Ritchie, 1987). Nevertheless, all voltage-gated Na^+ channels exposed to sufficient concentrations of these agents will be affected. This can explain why the accidental intravascular injection or the use of high concentrations of local anesthetics can produce profound systemic effects, especially in the central nervous and cardiovascular systems (Covino, 1987). Indeed, several local anesthetics also exhibit class I antiarrhythmic actions on the myocardium at lower concentrations than those used for local anesthesia (Grant et al., 1984; Bennett et al., 1995).

Bupivacaine is a potent local anesthetic widely used for long-lasting regional local anesthesia. In isolated cardiac tissues, bupivacaine decreases intracardiac conduction velocity and contractile force and depresses spontaneous sinoatrial activity (Block and Covino, 1982; Moller and Covino, 1988). In anesthetized animals, bupivacaine decreases cardiac output, myocardial contractility, and intracardiac conduction velocity as evidenced by increased PR and QRS durations (Covino, 1987; Liu et al., 1982). Furthermore, several studies have shown a correlation between cardiac sodium channel (I_{Na}) inhibition and depression of the cardiovascular system (Covino, 1987; Block and Covino, 1988). Although the high potency of bupivacaine to inhibit I_{Na} (Clarkson and Hondeghem, 1985) can partially explain its high cardiotoxicity, it has also been shown that bupivacaine induces a prolongation of the QTc interval of the ECG in anesthetized dogs (Avery et al., 1984; Wheeler et al., 1988; Solomon et al., 1989) and human volunteers (Scott et al., 1989) receiving high doses of bupivacaine. In some cases, this was accompanied by *torsades de pointes* (Kasten and Martin, 1985). These results suggest that the cardiotoxicity of bupivacaine also involves both block of Na^+ and K^+ channels, as it has been demonstrated (Valenzuela et al., 1995a;b). Ropivacaine, the S(–) enantiomer of AL381, which is chemically related to bupivacaine was synthetized as a less toxic alternative to bupivacaine. Although cardiotoxicity of this compound is lower than that previously reported to bupivacaine (Scott et al., 1989; Åkerman et al., 1988; Pitkanen et al., 1992), it has also been demonstrated that ropivacaine is able to induce the appearance of early-depolarizations in isolated preparations (Moller and Covino, 1990), probably secondary to a blockade of K^+

channels (Valenzuela et al., 1997).

IQB-9302 is a new amide type local anesthetic, chemically related to bupivacaine and synthetized as a less toxic alternative to bupivacaine and ropivacaine (Figure 1). Preliminary experiments have demonstrated that it is less cardiotoxic than bupivacaine (Gallego-Sandín et al., 1999). In order to test if IQB-9302 and its enantiomers block hKv1.5 channels similarly to bupivacaine, we have studied the effects of IQB-9302 on hKv1.5 channels. It will permit us to know if this drug would inhibit the native counterpart of this current (I_{Kur}) (Wang et al., 1993), since selective block of this current affects action potential duration in human atria (Wang et al., 1993). Therefore, the purpose of this study is to determine the mechanism of action of IQB-9302 on hKv1.5 channels expressed in a mammalian cell line (*Ltk*) without the complications of overlapping currents.

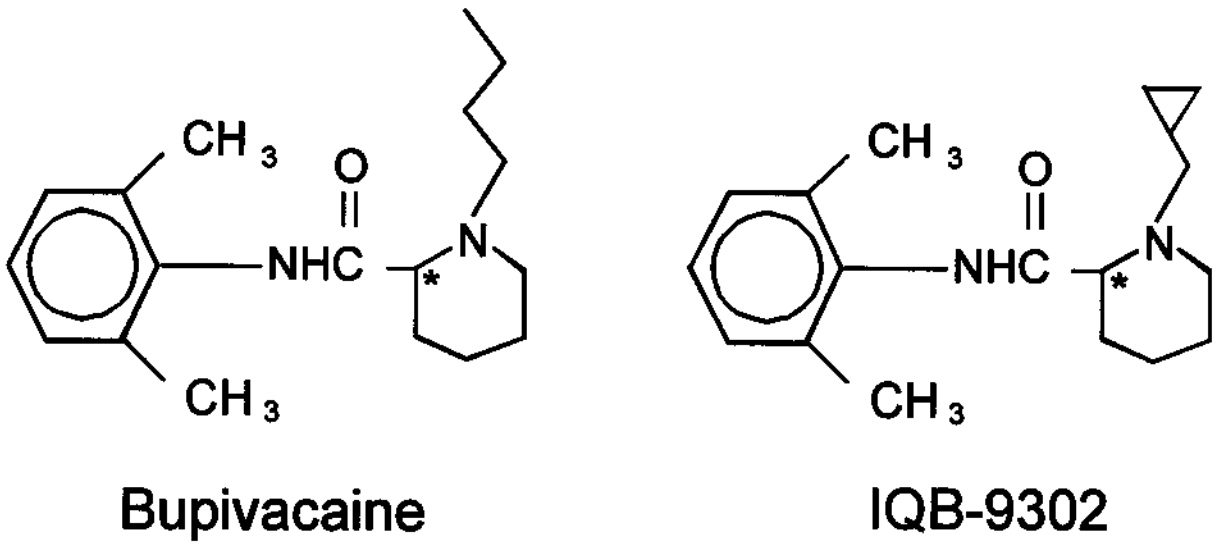

Figure 1. Chemical structure of bupivacaine and IQB-9302. The asterisk represents the asymmetric carbon.

Materials and Methods

Electrophysiological recording

Use of the stable *Ltk*⁻ cell line expressing hKv1.5 channels has been described previously in detail (Snyders et al., 1993, Valenzuela et al., 1995a; Franqueza et al., 1997; Longobardo et al., 1998). The intracellular pipette filling solution contained (in mM): K-aspartate 80, KCl 50, phosphocreatine 3, KH_2PO_4 10, MgATP 3, HEPES-K 10, EGTA 5 and was adjusted to pH 7.25 with KOH. The bath solution contained (in mM): NaCl 130, KCl 4, $CaCl_2$ 1.8, $MgCl_2$ 1, HEPES-Na 10, and glucose 10, and was adjusted to pH 7.40 with NaOH. Racemic IQB-9302, its enantiomers and racemic bupivacaine were dissolved in distilled deionized water to yield a stock solution of 10 mM from which further dilutions were made to obtain the desired final concentration. Experiments were performed in a small volume (0.5 ml) bath mounted on the stage of an inverted microscope (Nikon model TMS, Garden City, NY) perfused continuously at a flow rate of 0.5-1.0 ml/min. hKv1.5 currents were recorded at room temperature (20-22ºC) using the whole-cell voltage-clamp configuration of the patch-clamp technique (Hamill et al., 1981) with an Axopatch 1C patch-clamp amplifier (Axon Instruments, Foster City, CA). Currents were filtered at 2 kHz (four-pole Bessel filter), sampled at 4 kHz. Data acquisition and command potentials were controlled by the pCLAMP 6.0.1 software (Axon Instruments). Micropipettes were pulled from borosilicate glass capillary tubes (Narishige, GD-1, Tokyo, Japan) on a programmable horizontal puller (Sutter Instrument Co., San Rafael, CA) and heat-polished with a microforge (Narishige). When filled with the intracellular solution and immersed into the bath (external solution), the pipette tip resistance ranged between 1 and 3 MΩ. The micropipettes were gently lowered onto the cells to obtain a gigaohm seal (16±6 GΩ) after applying suction. After seal formation, cells were lifted from the bottom of the perfusion bath and the membrane patch was ruptured with brief additional suction. The capacitive transients elicited by symmetrical 10-mV steps from −80 mV were recorded at 50 kHz (filtered at 10 kHz) for subsequent calculation of capacitative surface area, access resistance, and input impedance. Thereafter, capacitance and series resistence compensation were optimized, and 80% compensation of the effective access resistance was usually obtained.

Pulse protocol and analysis

The holding potential was maintained at −80 mV unless indicated otherwise. After control data were obtained, bath perfusion was switched to drug-containing solution. The effects of drug infusion was monitored with test pulses to +60 mV, applied every 10 s until steady-state was obtained (after ~12 s). Steady-state current-voltage relationships (IV) were obtained by averaging the current over a small window (2-5 ms) at the end of 250 ms depolarizing pulses. Between −80 and −40 mV only passive linear leak was observed and least squares fits to these data were used for passive leak correction. Deactivating "tail" currents were recorded either at −40 mV. The activation curve was obtained from the tail current amplitude immediately after the capacitive transient. Measurements were done using the CLAMPFIT program of PCLAMP 6.0.1 and by a custom-made analysis program.

A first-order blocking scheme was used to describe drug-channel interaction. Apparent affinity constants, K_D, and Hill coefficients, n_H, were obtained from fitting of the fractional block, f, at various drug concentrations [D]:

$$f = 1 / [1 + (K_D / [D])^{n_H}] \quad (1)$$

and apparent rate constants for binding (k) and unbinding (l) were obtained from solving:

$$k \times [D] + l = 1 / \tau_B = \lambda \quad (2a)$$

$$l / k = K_D \quad (2b)$$

in which τ_B represents the time constant of the fast initial drug-induced current decay after activation from the holding potential to +60 mV. The activation kinetics of hKv1.5 channels have been described as a sigmoidal process (Snyders et al., 1993). However, in the present study and in order to describe the dominant time constant of this process and the effects of drugs on it, the latter part of the current was fitted to a single exponential, following a procedure previously described and used for the same purpose (White and Bezanilla, 1975; Snyders et al., 1993; Valenzuela et al., 1995; Delpón et al., 1996). On the other hand, deactivation and inactivation were fitted to a biexponential process. Thus, both processes were fitted to an equation of the form:

$$y = C + A_1\exp(-t/\tau_1) + A_2\exp(-t/\tau_2) + \ldots + A_n\exp(-t/\tau_n) \quad (3)$$

where τ_1, τ_2 ... τ_n are the system time constants, A_1, A_2 ... A_n are the amplitudes of each component of the exponential, and C is the baseline value. The voltage dependence of

activation curves were fitted with a Boltzmann equation: $y = 1/[1 + \exp(-(E-E_h)/s)]$, in which s represents the slope factor, E the membrane potential and E_h the voltage at which 50% of the channels are open. The curve-fitting procedure used a non-linear least-squares (Gauss-Newton) algorithm; results were displayed in linear and semilogarithmic format, together with the difference plot. Goodness of fit was judged by the χ^2 criterion and by inspection for systematic non-random trends in the difference plot.

Voltage dependence of block was determined as follows: leak-corrected current in the presence of drug was normalized to matching control to yield the fractional block at each voltage ($f = 1 - I_{drug}/I_{control}$). The voltage dependence of block was fitted to:

$$f = [D]/([D] + K_D^* \times \exp(-\delta zFE/RT)), \quad (4)$$

where z, F, R and T have their usual meaning, δ represents the fractional electrical distance, i.e., the fraction of the transmembrane electrical field sensed by a single charge at the receptor site and K_D^* represents the apparent dissociation constant at the reference potential (0 mV).

Statistical methods

Results are expressed as mean±SEM. Direct comparisons between mean values in control conditions and in the presence of drug for a single variable were performed by paired Student's t-test. Student's t-test was also used to compare two regression lines. Differences were considered significant if $P<0.05$.

Results

I. Effects induced by IQB-9302 enantiomers on hKv1.5 channels

Figure 2 shows original hKv1.5 current records obtained in the absence and in the presence of 50 μM S(−)IQB-9302 or R(+)IQB-9302 and after washout with drug-free external solution. The holding potential was maintained at -80 mV and 250 ms depolarizing pulses in duration to membrane potentials between -80 mV and +60 mV were applied. Tail currents were recorded upon repolarization to -40 mV. Under control conditions hKv1.5 current activates rapidly, reaches a maximum peak current and slowly inactivates, as previously described (Snyders et al., 1993). At 50 μM, both enantiomers inhibited hKv1.5 current, and R(+)IQB-9302 was more potent than the S(−) enantiomer (70.4±3.0%, n=4, *vs* 46.5±3.1%, n=10, $p<0.01$, respectively). The effects of both enantiomers were reversible upon perfusion of the cells with drug-free external solution (93±1% of the control values, n=23). S(−)IQB-9302 or R(+)IQB-9302 did not modify the activation kinetics of the current (1.28±0.11 ms *vs* 1.06±0.11 ms, n=8, $p>0.05$; and 1.73±0.20 ms *vs* 1.27±0.04, n=6, $p>0.05$; respectively). However, they induced, at high concentrations, a decline of the current at the beginning of the depolarizing pulse, which was faster at higher drug concentrations, suggesting an open channel block mechanism.

Figure 3 shows the concentration response curve when using as an index of block the suppression of the current induced by both enantiomers at +60 mV at the end of 250 ms depolarizing pulses. A non-linear least-squares fit of the concentration-response equation (see eq. 1 in Materials and Methods section) yielded, for S(−)IQB-9302, a K_D and the n_H values of 58.6±4.0 μM and 0.844±0.051, respectively. For R(+)IQB-9302, these values averaged 18.6±1.5 μM and 0.806±0.055. When n_H was fixed to unity, the K_D values for S(−)IQB-9302 and R(+)IQB-9302 were 57.6±5.0 μM ($p>0.05$) and 18.7±1.9 μM ($p>0.05$).

Voltage dependence of IQB-9302 induced block of hKv1.5 channels

Figure 4 shows the IV relationships obtained in the absence and in the presence of either S(−)IQB-9302 (50 μM) or R(+)IQB-9302 (10 μM). Both enantiomers decreased the amplitude of the current at all membrane potentials tested, although, the inhibition of the current was more pronounced at more positive than at more negative membrane potentials, thus

suggesting an open channel block mechanism similar to that described for bupivacaine, ropivacaine and mepivacaine enantiomers (Valenzuela et al., 1995a; 1997; Longobardo et al., 1998). In fact, both enantiomers induced a downward curvature of the IV relationship, indicating an open channel block mechanism. In order to quantitate this voltage dependence we represented the relative current in the presence of either 50 μM S(−)IQB-9302 or 10 μM R(+)IQB-9302 *versus* membrane potential. As it can be observed, block steeply increased in the range of membrane potentials of the activation of the channels, which indicates that the drug needs that the channel will open before it can bind. At membrane potentials positive to 0 mV a shallower but statistically significant increase in block was observed. Both enantiomers are weak bases (pKa=7.99±0.006) and thus, they are predominantly charged at the physiological pH. Thus, this increase in block can be attributed to the effect of the transmembrane electrical field on the interaction between the cationic form of the drug and the receptor at the channel. Following a Woodhull formalism (Woodhull, 1973) a non linear curve fitting of the data (see eq. 4 in the Materials and methods section) yielded apparent dissociation constant at the reference potential (0 mV) (K_D^*) and the fractional electrical distance from the inner side of the membrane (δ). In the presence of S(−)IQB-9302 and R(+)IQB-9302 the δ values averaged 0.173±0.022 (n=12) and 0.181±0.018 (n=10), respectively, indicating that they have to cross ~18% of the transmembrane electrical field to bind their receptor site in the hKv1.5 channel. In addition, the K_D^* averaged 78.8±26.3 μM (n=9) and 29.7±2.2 μM (n=10) for S(−)IQB-9302 and R(+)IQB-9302 , respectively.

Time dependent block

S(−) and R(+)IQB-9302 induced, at higher concentrations than 100 μM and 10 μM, respectively, a fast initial decline of the current which was superimposed to the slow inactivation (Figure 5A). The time constant of this fast decline of the current was lower at higher concentrations and thus, it was considered to be a good index of the time constant of block (τ_B). From the values of τ_B we calculated the apparent drug association (k) and dissociation (l) kinetics constants (see eq. 2 in Materials and Methods). In the case of S(−)IQB-9302, these kinetic constants reached mean values of 0.60±0.08 $\mu M^{-1}\ s^{-1}$ and 39.7±5.2 s^{-1} (n=13), respectively. For R(+)IQB-9302, k was 4.8-fold higher than that obtained for

S(-)IQB-9302 (2.90±0.63 μM^{-1} s^{-1}, n=7, $p<0.01$) whereas *l* was similar than that obtained with S(-)IQB-9302 (52.2±11.4 s^{-1}, n=7, $p>0.05$). Time dependent block was also observed in the deactivating process.

Figure 5B shows superimposed current traces obtained on return to –40 mV under control conditions and in the presence of S(-)IQB-9302 (20 μM) or R(+)IQB-9302 (10 μM). Under control conditions, the deactivating process was fitted following a biexponential process with an slow (τ_s) and a fast (τ_f) time constants. S(-)IQB-9302 increased the two time constants from 17.9±3.3 ms and 58.6±12.3 ms to 31.2±4.0 ms (n=5, $p<0.05$) and 167.4±30.4 ms (n=5, $p<0.05$). R(+)IQB-9302 increased the two process of deactivation from 18.7±2.9 ms and 48.4±6.5 ms to 28.0±5.0 ms (n=5, $p<0.05$) and 73.0±8.6 ms (n=5, $p<0.05$). Moreover, tail currents recorded in the presence of IQB-9302 enantiomers exhibited an initial rising phase that indicates drug dissociation from the blocked open channels. Subsequently, the tail current displays a slower decline because some fraction of the open channels become blocked again, rather than closing. These effects produced a "crossover" phenomenon when the tail currents obtained under control conditions and in the presence of the drug are superimposed, an indicator of open channel block (Armstrong, 1971).

II. Effects of racemic IQB-9302 and bupivacaine on hKv1.5 channels.

Figure 6 shows current records obtained in the absence and in the presence of 20 μM racemic IQB-9302 or bupivacaine and after washout with drug-free external solution. The holding potential was maintained at -80 mV and 250 ms depolarizing pulses in duration to membrane potentials between -80 mV and +60 mV were applied. Tail currents were recorded upon repolarization to -40 mV. At 20 μM, both drugs inhibited hKv1.5 current, being bupivacaine more potent than IQB-9302 (57.3±2.9%, n=4, *vs* 41.6±2.2%, n=10, $p<0.05$, respectively). The effects of both drugs were reversible upon perfusion of the cells with drug-free external solution (90±3% of the control values, n=21). Both drugs significantly accelerated the activation kinetics of the current (1.28±0.11 ms *vs* 0.81±0.09 ms, n=4, $p<0.01$; and 1.45±0.10 ms *vs* 1.19±0.11, n=4, $p<0.05$; for IQB-9302 and bupivacaine, respectively). Also, they induced a decline of the current at the beginning of the depolarizing pulse, which was faster at higher drug concentrations, suggesting an open channel block

mechanism.

As in the case of the enantiomers of IQB-9302, block induced by racemic IQB-9302 and bupivacaine was concentration dependent. Figure 7 shows the concentration response curve when using as an index of block the suppression of the current induced by both enantiomers at +60 mV at the end of 250 ms depolarizing pulses. A non-linear least-squares fit of the concentration-response equation (see eq. 1 in Materials and Methods section) yielded K_D and the n_H values of 8.6±4.0 μM and 0.751±0.086, for bupivacaine, and 18.8±4.1 μM and 0.658±0.110, for IQB-9302, respectively. When n_H was fixed to unity, the K_D values for bupivacaine and IQB-9302 were 8.9±1.4 μM ($p>0.05$) and 21.5±4.7 μM ($p>0.05$).

Voltage dependent block of hKv1.5 channels induced by racemic bupivacaine and IQB-9302

Figure 8 shows the IV relationships for hKv1.5 obtained in the absence and in the presence of bupivacaine or IQB-9302. As previously observed in the presence of the IQB-9302 enantiomers and reported for bupivacaine enantiomers (Valenzuela et al., 1995a), the degree of block induced by the racemic forms of bupivacaine and IQB-9302 was higher at more positive membrane potentials, suggesting an open channel block mechanism. In order to quantitate this voltage dependence the relative current in the presence of bupivacaine or IQB-9302 was plotted (Figure 8b). Similarly to that observed in the presence of IQB-9302 enantiomers, block steeply increased in the activation range of hKv1.5 channels (dotted line) and it significantly increased in a shallower way at membrane potentials positive to 0 mV. This voltage dependence was explained as in the case of bupivacaine and IQB-9302 enantiomers following a Woodhull formalism which let us to calculate the δ and the K_D^* values. These parameters averaged 0.213±2.3 and 20.4±2.3 μM (n=14) for bupivacaine. For IQB-9302, these values were 0.172±0.014 and 42.6±3.5 μM (n=9).

Time dependent block

Both drugs, IQB-9302 and bupivacaine, induced a fast initial decline of the current which was superimposed to the slow inactivation (Figure 9A), although the time dependent decay of the current was more evident in the presence of bupivacaine than in the presence of IQB-9302, reflecting a different association and dissociation kinetics for both drugs. In the

presence of IQB-9302 and bupivacaine this fast decline appeared at concentrations higher than 50 μM and 10 μM, respectively. The time constant of this fast decline of the current was lower at higher concentrations and thus, it was considered to be a good index of the kinetics of binding of the drug (τ_B). From the values of τ_B we calculated the apparent drug association (*k*) and dissociation (*l*) kinetics constants (see eq. 2 in Materials and Methods). In the case of IQB-9302, these kinetic constants reached mean values of 2.3±0.2 μM^{-1} s^{-1} and 59.1±5.9 s^{-1} (n=10), respectively. For bupivacaine, *k* was similar than that obtained for IQB-9302 (2.2±0.3 μM^{-1} s^{-1}, n=16, $p>0.01$) whereas *l* decreased 5.8-fold than that obtained with IQB-9302 (10.2±0.3 s^{-1}, n=16, $p<0.01$), that suggests a much more stable drug-channel complex. Time dependent block was also observed in the deactivating process. Figure 9b shows superimposed current traces obtained under control conditions and in the presence of IQB-9302 (20 μM) or bupivacaine (20 μM). Under control conditions, the deactivating process was fitted following a biexponential process with an slow (τ_s) and a fast (τ_f) time constants. IQB-9302 increased the two time constants from 19.0±3.3 ms and 57.9±15.0 ms to 28.2±2.9 ms (n=5, $p<0.05$) and 112.5±33.0 ms (n=5, $p>0.05$). In the absence of bupivacaine, deactivation process of hKv1.5 current exhibited a biexponential decay with τ_f=22.8±1.6 ms and τ_s=95.9±22.6 ms. Bupivacaine eliminated the fast component of deactivation which became a monoexponential process with a time constant of 97.2±19.2 ms (n=5, $p>0.05$ *versus* the slow time constant observed under control conditions). Moreover, in the presence of both IQB-9302 or bupivacaine, there was an initial rising phase at the beginning of the tail current, that indicates the dissociation of the drug from the receptor at the channel. The slowing of the deactivating process induced by both drugs produced a "crossover" phenomenon when the tail currents obtained under control conditions and in the presence of the drug are superimposed and this phenomenon is an indicator of open channel block (Armstrong, 1971).

Discussion

The main findings of the present study are: 1) IQB-9302 induced block of hKv1.5 channels is stereoselective, 2) both enantiomers of this new local anesthetic block the open state of hKv1.5 channels and 3) the stereoselectivity observed for the IQB-9302 enantiomers is due to the spatial localization of the N-substituent of the molecule, as well as that observed for ropivacaine and bupivacaine (Valenzuela et al., 1997; Longobardo et al., 1998).

IQB-9302, its enantiomers and bupivacaine block the open state of hKv1.5 channels

There are several pieces of evidence suggesting that IQB-9302, its enantiomers as well as racemic bupivacaine block hKv1.5 channels by binding to the open state. First, all these drugs, at enough high concentrations, induce a fast initial decline of the maximal activated current, that superimposes to the intrinsic C-type inactivation of these channels. Second, block steeply increased in the range of activation of the hKv1.5 channels activation, indicating that the drug need that the channel opens to bind to its receptor site and block the K^+ efflux. For all drugs studied block was also voltage dependent at membrane potentials positive to 0 mV and this voltage dependence was shallower than that observed in the activation range of hKv1.5 channels. This effect was explained following a Woodhull model (Woodhull, 1973), which led us to calculate the fractional electrical distance from the inside of the membrane (δ~0.19 for both enantiomers). Finally, when the tail currents obtained in the absence and in the presence of each drug were superimposed, we observed a tail current "crossover" as a consequence of an slowing of the time course of deactivation of the current and which is a reflect of an open channel block mechanism (Armstrong, 1971; Follmer et al., 1990; Snyders et al., 1992; Valenzuela et al., 1995; 1997; Longobardo et al., 1998).

Affinity related to the length between the tertiary amine and the end of the N-substituent

Bupivacaine, ropivacaine, IQB-9302 and mepivacaine are local anesthetics which only differ in the N-substituent which is a n-butyl, n-propyl, cyclopropylmethyl and methyl, respectively. In order to quantitate the relationship between the affinity and the length of the N-substituent we have measured the maximal length between the tertiary amine and the end of the substituent and we have represented the $\log K_D$ *vs* the maximal length (in Å) (Figure 10).

For each pair of enantiomers, there was a good linear relationship between the potency and the length of the N-substituent group, suggesting that this region of the molecule determines the potency of the drug.

Stereoselective block of hKv1.5 channels induced by IQB-9302

Block induced by IQB-9302 was stereoselective. As previously described with bupivacaine (Valenzuela et al., 1995a), the R(+) enantiomer was the more potent, although for IQB-9302, the degree of stereoselective block was lower than that observed for bupivacaine, in which case, the R(+) enantiomer was 7-fold more potent that S(−)bupivacaine, whereas R(+)IQB-9302 was 3.1 more potent than S(−)IQB-9302. For the enantiomers of these two drugs, as well as for those of ropivacaine, the difference in potency between both enantiomers was related to the faster association rate constant of the R(+) enantiomers. Stereoselective interactions suggest that unidirectional structural properties of the side chain such as hydrophobicity (logP) or van der Waals volume (Vw) cannot be the main responsible for the differences in potency (Figure 10). In contrast, it seems to be the consequence of some stereochemical property of the drug, such as the length of the N-substituent, which would adopt opposite spatial localization for each pair of enantiomers.

To further analyze this issue, the minimum energy conformers of the N-protonated bupivacaine (N-n-butyl), ropivacaine (N-n-propyl), IQB-9302 (N-cyclopropylmethyl) and mepivacaine (N-methyl) were modeled using the Hyperchem program. The cationic forms were selected because all these drugs are weak bases (with pKa values ≈8) and, therefore, they will be mostly protonated at the physiological pH. This analysis was carried out both for S(−) and R(+) enantiomers and docking of the conformers of minimum energies were performed in order to explore sterical differences. Figure 11A and 11C shows the two enantiomers of bupivacaine superimposed by the piperidine ring. As we can observe, under these circumstances, both enantiomers almost fit completely, which does not explain the experimental differences in potency for the enantiomers of bupivacaine and IQB-9302, respectively (Valenzuela et al., 1995a). Figure 11B and 11D show the S(−) and R(+) enantiomers of bupivacaine and IQB-9302 superimposed by their aromatic rings. In this case, it can be observed that, for both drugs, S(−) and R(+) enantiomers differ in the position of the N-

substituents, which are in opposite directions for each enantiomer, which could explain the observed differences in potency. According to Figure 10, R(+) enantiomers adopt a more favorable conformation in energetic terms than the S(-) enantiomers, that explain their higher potency. This simple approach lead us to propose a recognition model for this type of local anesthetics (Valenzuela et al., 1995[a]; 1997; Longobardo et al., 1998), suggesting a restrictive site for the recognition of the aromatic ring. Under this hypothesis, first, the aromatic ring of the drug would interact with an amino acid containing an aromatic ring (Phe, Tyr or Trp) establishing a π-π interaction between both aromatic rings. Afterwards, the N-substituent would interact with some of the two amino acids (L508 and V512) previously identified as part of the receptor site for bupivacaine in hKv1.5 channels (Franqueza et al., 1997).

Effects of racemic IQB-9302 and bupivacaine on hKv1.5 channels.

The racemic forms of IQB-9302 and bupivacaine inhibit hKv1.5 currents by binding to the open state of hKv1.5 channels, as it can be derived from the time- and voltage-dependent effects. In fact, the characteristics of the blockade of IQB-9302 are very similar to those exhibited by its enantiomers, being its potency closer to the R(+), more potent, enantiomer. Similarly, the characteristics of the racemic bupivacaine hKv1.5 induced block are very close to that observed with IQB-9302 enantiomers and its potency was very similar to that induced by R(+)bupivacaine.

The lower potency of IQB-9302 can be attributed to a faster dissociation rate constant, i.e., to a more unstable drug-channel complex. Table 1 shows the K_D, k and l values obtained for bupivacaine enantiomers, IQB-9302 enantiomers, ropivacaine enantiomers and racemic IQB-9302 and bupivacaine. For all pairs of enantiomers, block of hKv1.5 channels was stereoselective, with the higher degree of stereoselectivity for bupivacaine and a similar stereoselective block for ropivacaine and IQB-9302, that is likely due to the similar length of the side chain of the N-substituent. A low affinity of a local anesthetic for hKv1.5 is, in principle, a good index between the therapeutic and the toxic effects, since the pharmacological target of local anesthetics are not K^+ channels, but the Na^+ channels. Thus, the ideal local anesthetic in terms of blocking effects of Na^+ and K^+ channels, would be that one which would exhibit a much higher affinity for Na^+ channels than for K^+ channels.

Our results suggest that both the racemic and the S(–) enantiomer of IQB-9302 exhibit a more promising pharmacological profile than racemic bupivacaine and similar to that observed with S(–)bupivacaine and ropivacaine in terms of potassium channel blockade. Further experiments in which the effects of racemic and the enantiomers of IQB-9302 on ventricular K^+ currents as well as on cardiac and neuronal Na^+ currents are needed to know the pharmacological differences between these compounds, as well as the possible benefits of the development of either the racemic or some of the IQB-9302 enantiomers.

References

Akerman B, Hellberg I and Trossvik C (1988) Primary evaluation of the local anaesthetic properties of the amino amide agent ropivacaine (LEA 103). *Acta Anaesthesiol Scand* **32**:571-578.

Armstrong CM (1971) Interaction of tetraethylammonium ion derivatives with the potassium channels of giant axons. *J Gen Physiol* **58**:413-437.

Avery P, Redon D, Schaenzer G, Rusy B (1984) The influence of serum potassium on the cerebral and cardiac toxicity of bupivacaine and lidocaine. *Anesthesiology* **61**:134-138.

Bennett PB, Valenzuela C, Chen L-Q, Kallen R (1995) On the molecular nature of the lidocaine receptor of cardiac Na^+ channels: Modification of block by alterations in the α-subunit III-IV interdomain. *Circ Res* **77**:584-592.

Block, A and Covino, BG (1982) Effects of local anesthetic agents on cardiac conduction and contractility. *Reg Anesth* **6**:55-61.

Clarkson C and Hondeghem L (1985) Evidence for a specific receptor site for lidocaine, quinidine and bupivacaine associated with cardiac sodium channels in guinea-pig ventricular myocardium. *Circ Res* **56**:496-506.

Covino B (1987) Toxicity and systemic effects of local anesthetic agents. In: G. Strichartz ed. *Local Anesthetics Handbook of Experimental Pharmacology*, Vol. 81, Heidelberg, Springer-Verlag, pp. 187-212.

Delpón E, Valenzuela C, Perez O, Franqueza L, Gay P, Snyders DJ and Tamargo J (1996) Mechanisms of block of a human cloned potassium channel by the enantiomers of a new bradycardic agent: S-16257-2 and S-16260-2. *Br J Pharmacol* **117**:1293-1301.

Follmer C, Cullinan C and Coltasky (1992) Differential block of cardiac delayed rectifier current by class Ic antiarrhythmic drugs: evidence for open channel block and unblock. *Cardiovasc Res* **26**:1121-1130.

Franqueza L, Longobardo M, Vicente J, Delpón E, Tamkun MM, Tamargo J, Snyders DJ and Valenzuela C (1997) Molecular determinants of stereoselective bupivacaine block of hKv1.5 channels. *Circ Res* **81**:1053-1064.

Gallego-Sandín S, Novalbos J, Gálvez-Múgica MA, García AG and Abad F (1999) Comparison of hemodynamic effects of IQB-9302 and bupivacaine in anesthetized rats. *Meth Find Exp Clin Pharmacol* **21**:158.

Grant A, Starmer C and Strauss H (1990) Antiarrhythmic drug action: blockade of inward current. *Circ Res* **55**:427-439.

Hamill O, Marty A, Neher E, Sakmann B and Sigworth F (1981) Improved patch-clamp techniques for high resolution current recording from cells and cell-free membrane patches. *Pflügers Archiv* **391**:85-100.

Hille B (1977) Local anesthetics: Hydrophilic and hydrophobic pathways for the drug-receptor reaction. *J Gen Physiol* **69**:497-515.

Hondeghem L and Katzung B (1977) Time- and voltage-dependent interactions of antiarrhythmic drugs with cardiac sodium channels. *Biochim Biophys Acta* **472**:373-398.

Kasten G and Martin S (1985) Bupivacaine cardiovascular toxicity: Comparison of treatment with bretylium and lidocaine. *Anesth Analg* **64**:911-916.

Liu, P, Feldman, HS, Covino, BM, Giasi, R and Covino, BG (1982) Acute cardiovascular toxicity of intravenous amide local anesthetics in anesthetized ventilated dogs. *Anesth Analg*

61:317-322.

Longobardo M, Delpón E, Caballero R, Tamargo J and Valenzuela C (1998) Structural determinants of potency and stereoselective block of hKv1.5 channels induced by local anesthetics. *Mol Pharmacol* **54**:162-169.

Moller R and Covino B (1990) Cardiac electrophysiologic properties of bupivacaine and lidocaine compared with those of ropivacaine, a new amide local anesthetic *Anesthesiology* **72**:322-329.

Pitkanen, M, Feldman, HS, Arthur, GR and Covino, BG (1992) Chronotropic and inotropic effects of ropivacaine, bupivacaine, and lidocaine in the spontaneously beating and electrically paced isolated, perfused rabbit heart. *Reg Anesth* **17**:183-192.

Scott B, Lee A, Fagan D, Bowler G, Bloomfield P and Lundh R (1989) Acute toxicity of ropivacaine compared with that of bupivacaine. *Anesth Analg* **69**:563-569.

Snyders D, Knoth K, Roberds S and Tamkun M (1992) Time-, state- and voltage-dependent block by quinidine of a cloned human cardiac channel. *Mol Pharmacol* **41**:332-339.

Snyders DJ, Tamkun MM and Bennett PB (1993) A rapidly activating and slowly inactivating potassium channel cloned from human heart. Functional analysis after stable mammalian cell culture expression. *J Gen Physiol* **101**:513-543.

Solomon D, Bunegin L and Albin M (1990) The effect of magnesium sulfate administration on cerebral and cardiac toxicity of bupivacaine in dogs. *Anesthesiology* **72**:341-346.

Strichartz GR (1987) Local Anesthetics, Springer-Verlag, Berlin Heidelberg.

Strichartz GR and Ritchie JM (1987) The action of local anesthetics on ion channels of

excitable tissues, in Local Anesthetics (Strichartz GR, ed), pp 21-52, Springer Verlag, Berlin, Germany.

Valenzuela C, Delpón E, Tamkun MM, Tamargo J and Snyders DJ (1995a) Stereoselective block of a human cardiac potassium channel (Kv1.5) by bupivacaine enantiomers. *Biophys J* **69**:418-427.

Valenzuela C, Snyders DJ, Bennett PB, Tamargo J and Hondeghem LM (1995b) Stereoselective block of cardiac sodium channels by bupivacaine in guinea pig ventricular myocytes. *Circulation* **92**:3014-3024.

Valenzuela C, Delpón E, Franqueza L, Gay P, Snyders D and Tamargo J (1997) Effects of ropivacaine on a potassium channel (hKv1.5) cloned from human ventricle. *Anesthesiology* **86**:718-728.

Wang Z, Fermini B and Nattel S (1993) Sustained depolarization-induced outward current in human atrial myocytes. Evidence for a novel delayed K^+ current similar to Kv1.5 cloned channel currents. *Circ Res* **73**:1061-1076.

Wheeler D, Bradley E and Woods W (1988) The electrophysiologic actions of lidocaine and bupivacaine in the isolated, perfused canine heart. *Anesthesiology* **68**:201-212.

White M and Bezanilla F (1985) Activation of squid axon K^+ channels: ionic and gating current studies. *J Gen Physiol* **85**:539-554.

Woodhull AM (1973) Ionic blockade of sodium channels in nerve. *J Gen Physiol* **61**:687-708.

Table 1. Values of K_D, k and l for bupivacaine, ropivacaine and IQB-9302 enantiomers and racemic bupivacaine and IQB-9302.

	K_D (μM)	k ($\mu M^{-1} s^{-1}$)	l (s^{-1})
*R(+)bupivacaine	4	4.5	23
*S(−)bupivacaine	27	1	23
*R(+)ropivacaine	32	1.5	48
*S(−)ropivacaine	81	0.5	40
R(+)IQB-9302	19	2.9	52
S(−)IQB-9302	65	0.6	39
(R,S)bupivacaine	8	2.2	10
(R,S)IQB-9302	21	2.3	59

Values for ropivacaine and bupivacaine enantiomers are taken from previous studies (Valenzuela et al., 1995a; 1997; Longobardo et al., 1998).

Figure Legends

Figure 1. Chemical structure of bupivacaine and ropivacaine. The asterisk indicates the asymmetric carbon in the molecule.

Figure 2. Effects of IQB-9302 enantiomers on hKv1.5 currents. Currents are shown for depolarizations from −80 mV to voltages between −80 and +60 mV in steps of 10 mV. Tail currents were obtained on return to −40 mV. All records shown in this figure were recorded from the same cell, which was first perfused with S(−)IQB-9302 (top panels) and afterwards with R(+)IQB-9302 (bottom panels). The control for R(+)IQB-9302 is the washout of S(−)IQB-9302. Cell capacitance, 23 pF. Data filtered at 2 kHz (four-pole Bessel) and digitized at 10 kHz; additional digital filtering at 1 kHz.

Figure 3. Concentration dependence of IQB-9302 enantiomers-induced block of hKv1.5 channels. Reduction of current (relative to control) at the end of depolarizing steps from −80 mV to +60 mV was used as index of block. Data are mean±SEM of a total of 51 experiments. The continuous line represents the fit of the experimental data to the equation: $1/[1+(K_D/[D])^{n_H}]$.

Figure 4. Voltage dependence of hKv1.5 block by IQB-9302 enantiomers. **Panel A**: Current-voltage relationship in control conditions (●) and in the presence of 50 μM S(−)IQB-9302 (○). **Panel B**: Relative current expressed as $I_{S(-)IQB\text{-}9302}/I_{Control}$ from data shown in panel A. **Panel C**: Current-voltage relationship in control conditions (●) and in the presence of 10 μM R(+)IQB-9302 (○). **Panel D**: Relative current expressed as $I_{R(+)IQB\text{-}9302}/I_{Control}$ from data shown in panel C. The dashed lines in panels B and D represent the activation curve of the hKv1.5 channel for each experiment. In both cases, block increased steeply between −20 mV and 0 mV, which corresponds to the voltage range of activation of hKv1.5. For membrane potentials positive to 0 mV, a continued but more shallow voltage dependence was observed. This voltage dependence was fitted (continuous line) with eq. 4 (see Materials and Methods) and yielded $\delta \sim 0.18$.

Figure 5. Time dependent block induced by IQB-9302 enantiomers. **Panel A**: Superimposed traces for steps from −80 mV to +60 mV recorded under control conditions and in the presence of 500 μM S(−)IQB-9302 and 50 μM R(+)IQB-9302. **Panel B**: Tail current crossover. Superimposed tail currents recorded on return to −40 mV, in control conditions and

in the presence of 20 μM S(-)IQB-9302 or 10 μM R(+)IQB-9302. *Arrow* shows the crossover of tracings recorded in the presence of IQB-9302 enantiomers with those recorded under control conditions.

Figure 6. Effects of racemic IQB-9302 and bupivacaine on hKv1.5 currents. Currents are shown for depolarizations from −80 mV to voltages between −80 and +60 mV in steps of 10 mV. Tail currents were obtained on return to −40 mV. All records shown in this figure were recorded from the same cell, which was first perfused with 20 μM bupivacaine (top panels) and afterwards with 20 μM IQB-9302 (bottom panels). The control for IQB-9302 is the washout of bupivacaine. Cell capacitance, 22 pF. Data filtered at 2 kHz (four-pole Bessel) and digitized at 10 kHz; additional digital filtering at 1 kHz.

Figure 7. Concentration dependence of racemic IQB-9302 and bupivacaine-induced block of hKv1.5 channels. Reduction of current (relative to control) at the end of depolarizing steps from −80 mV to +60 mV was used as index of block. Data are mean±SEM of a total of 51 experiments. The continuous line represents the fit of the experimental data to the equation: $1/[1+(K_D/[D])^{n_H}]$.

Figure 8. Voltage dependence of hKv1.5 block by racemic IQB-9302 and bupivacaine. **Panel A**: Current-voltage relationship in control conditions (○) and in the presence of 20 μM IQB-9302 (●) or 20 μM bupivacaine (▲). **Panel B**: Relative current expressed as $I_{Drug}/I_{Control}$ from data shown in panel A. The dashed line in panel B represents the activation curve of the hKv1.5 channel. For both drugs, block increased steeply between −20 mV and 0 mV, which corresponds to the voltage range of activation of hKv1.5. For membrane potentials positive to 0 mV, a continued but more shallow voltage dependence was observed. This voltage dependence was fitted (continuous line) with eq. 4 (see Materials and Methods) and yielded $\delta \sim 0.17$.

Figure 9. Time dependent block induced by racemic IQB-9302 and bupivacaine. **Panel A**: Superimposed traces for steps from −80 mV to +60 mV recorded under control conditions and in the presence of 20 μM IQB-9302 and 20 μM bupivacaine. **Panel B**: Tail current crossover. Superimposed tail currents recorded on return to −40 mV, in control conditions and in the presence of 20 μM IQB-9302 or 20 μM bupivacaine. *Arrow* indicates the "crossover" of

tracings recorded in the presence of both drugs with those recorded under control conditions.

Figure 10. Relationship between the potency of block of hKv1.5 channels and the maximal length between the tertiary amine and the end of the N-substituent of the enantiomers of mepivacaine, IQB-9302, ropivacaine and bupivacaine.

Figure 11. Minimum energy conformers of the two enantiomers of bupivacaine (left panels) and IQB-9302 (right panels) superimposed by the piperidine ring (**panels A** and **B**) or by the aromatic ring (**panels C** and **D**). In both cases, the R(+) enantiomers are shown with thicker lines than the S(-) ones. Note that only when each pair of enantiomers are superimposed by the aromatic ring a difference in the spatial configuration of the drugs can explain the experimental differences in potency. Both models were constructed by using the Hiperchem program.

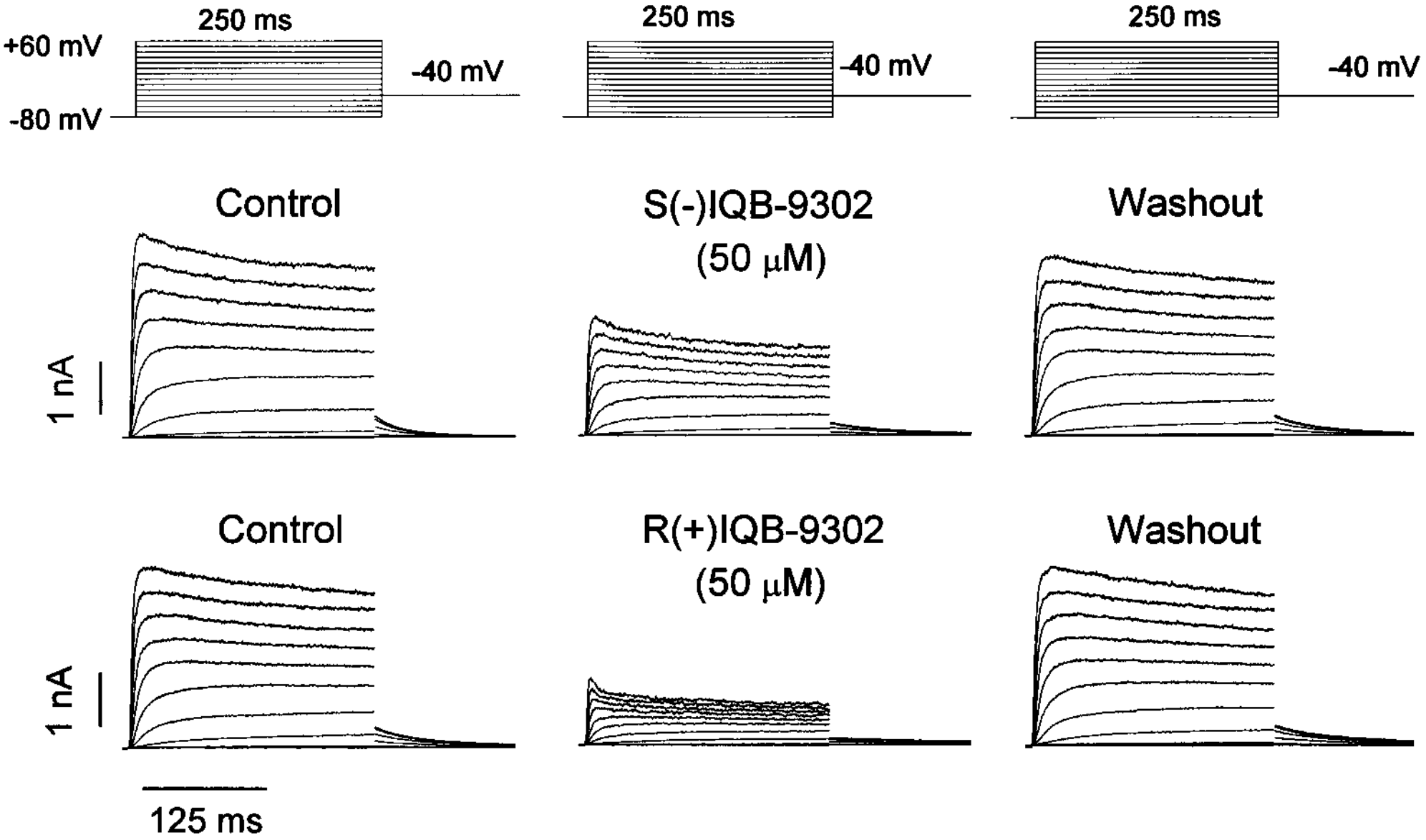
250 ms
+60 mV
-80 mV
-40 mV
250 ms
-40 mV
250 ms
-40 mV
Control
S(-)IQB-9302
(50 μM)
Washout
1 nA
Control
R(+)IQB-9302
(50 μM)
Washout
1 nA
125 ms

Figure 2

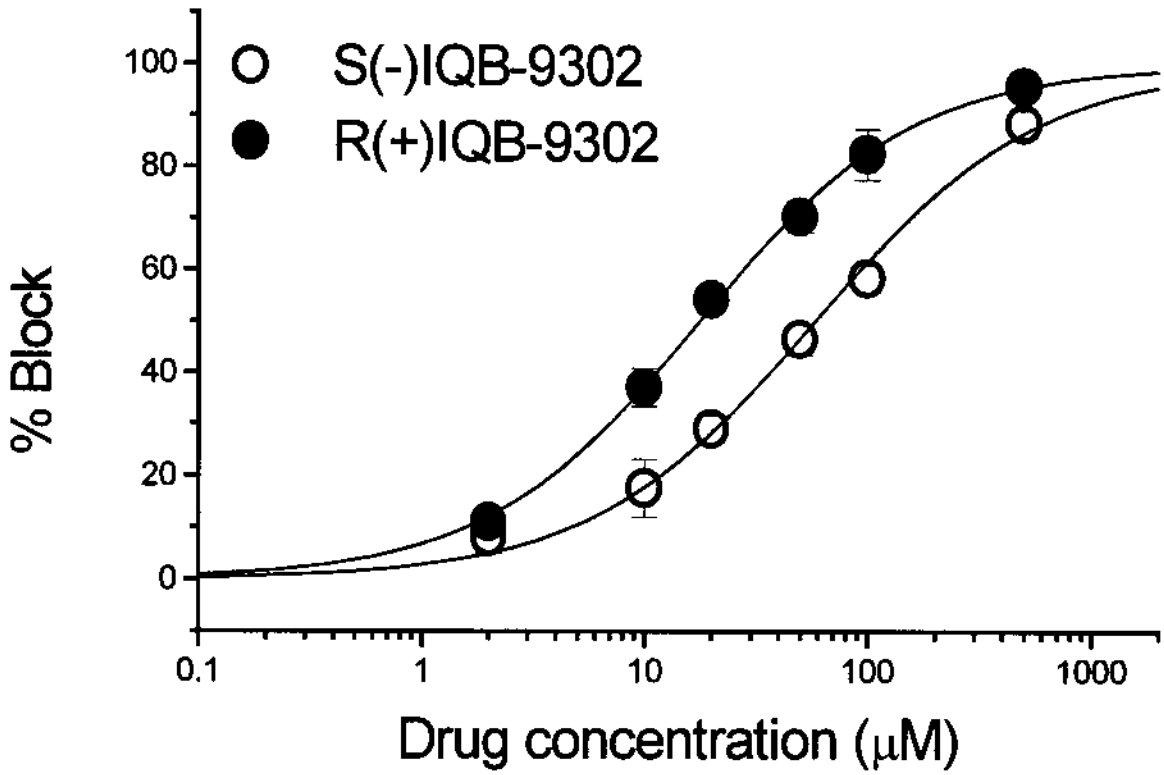
S(-)IQB-9302
R(+)IQB-9302
% Block
100
80
60
40
20
0
0.1
1
10
100
1000
Drug concentration (μM)

Figure 3

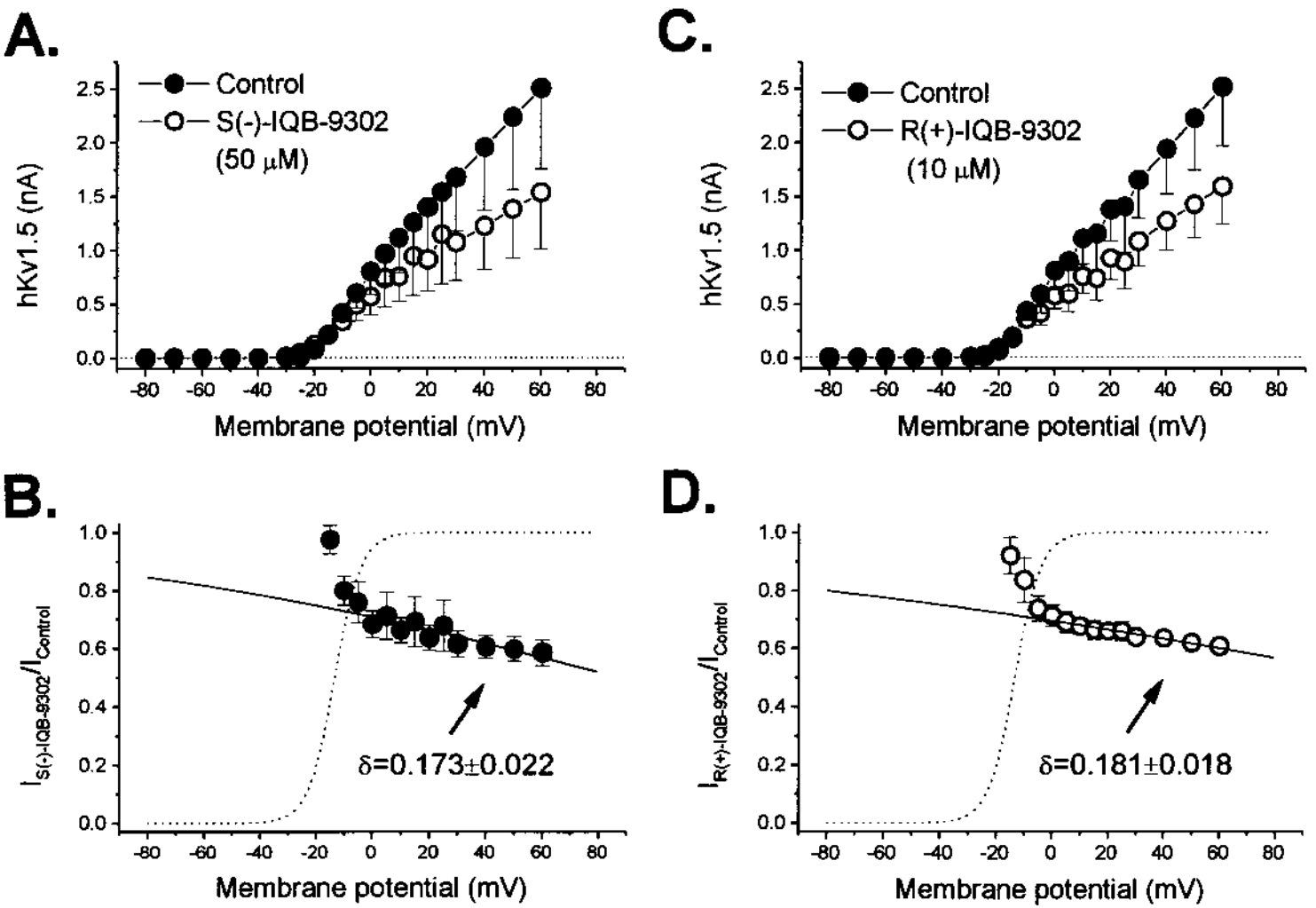
A.
Control
S(-)-IQB-9302
(50 μM)
hKv1.5 (nA)
Membrane potential (mV)
C.
Control
R(+)-IQB-9302
(10 μM)
hKv1.5 (nA)
Membrane potential (mV)
B.
$I_{S(-)\text{-}IQB\text{-}9302}/I_{Control}$
δ=0.173±0.022
Membrane potential (mV)
D.
$I_{R(+)\text{-}IQB\text{-}9302}/I_{Control}$
δ=0.181±0.018
Membrane potential (mV)

Figure 4

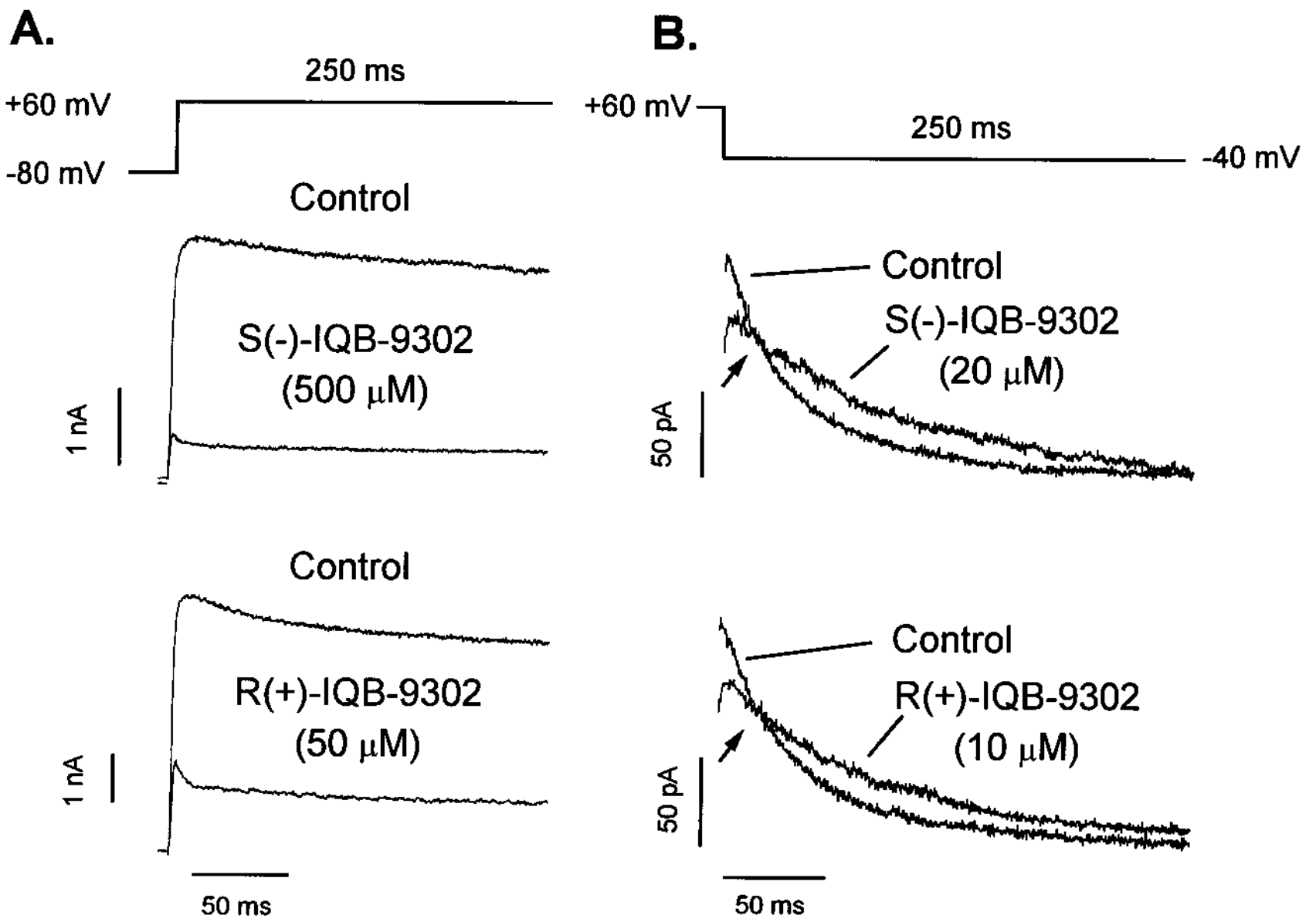
A.
250 ms
+60 mV
-80 mV
Control
S(-)-IQB-9302
(500 μM)
1 nA
Control
R(+)-IQB-9302
(50 μM)
1 nA
50 ms
B.
+60 mV
250 ms
-40 mV
Control
S(-)-IQB-9302
(20 μM)
50 pA
Control
R(+)-IQB-9302
(10 μM)
50 pA
50 ms

Figure 5

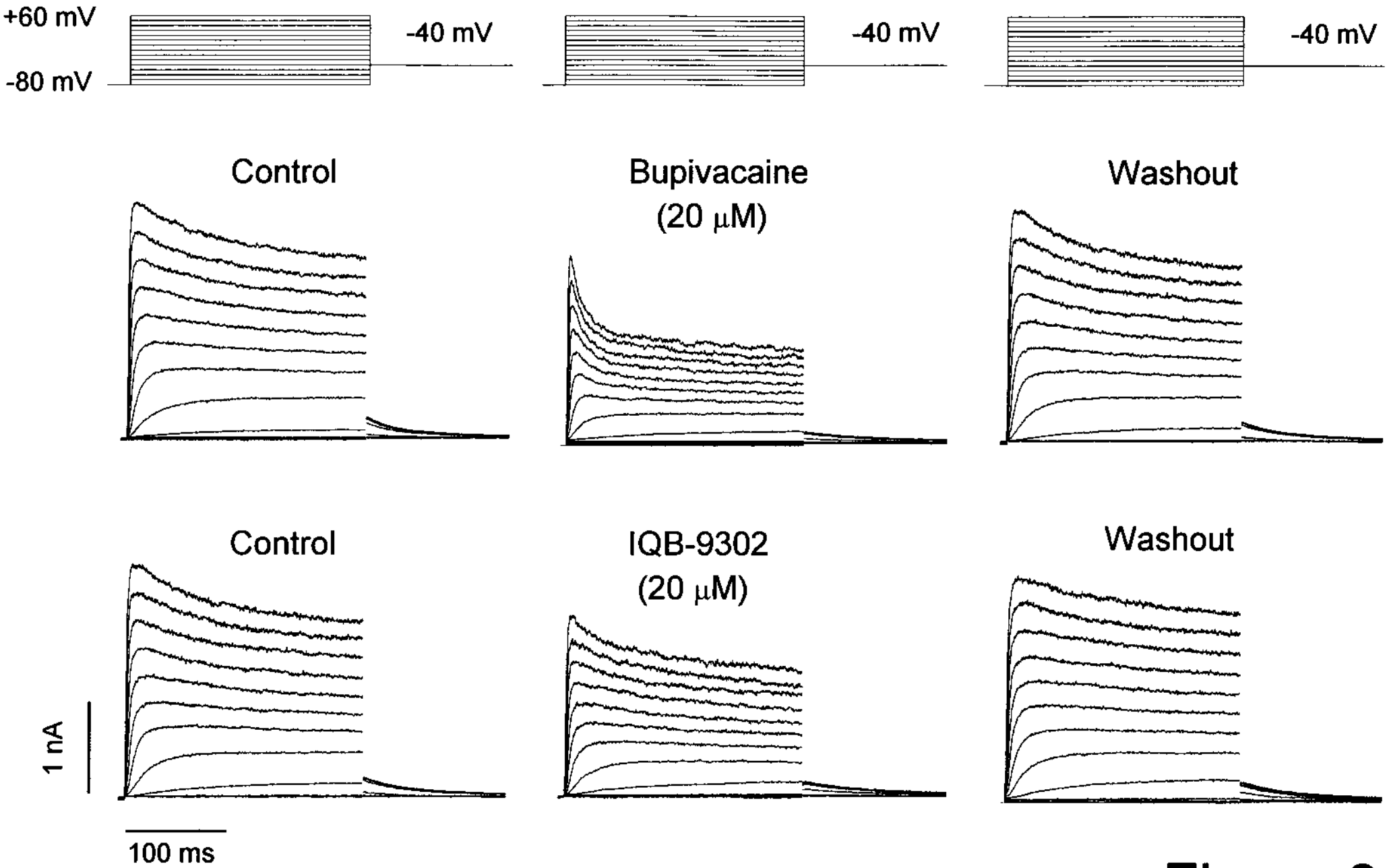
+60 mV
-80 mV
-40 mV
-40 mV
-40 mV
Control
Bupivacaine
(20 μM)
Washout
Control
IQB-9302
(20 μM)
Washout
1 nA
100 ms

Figure 6

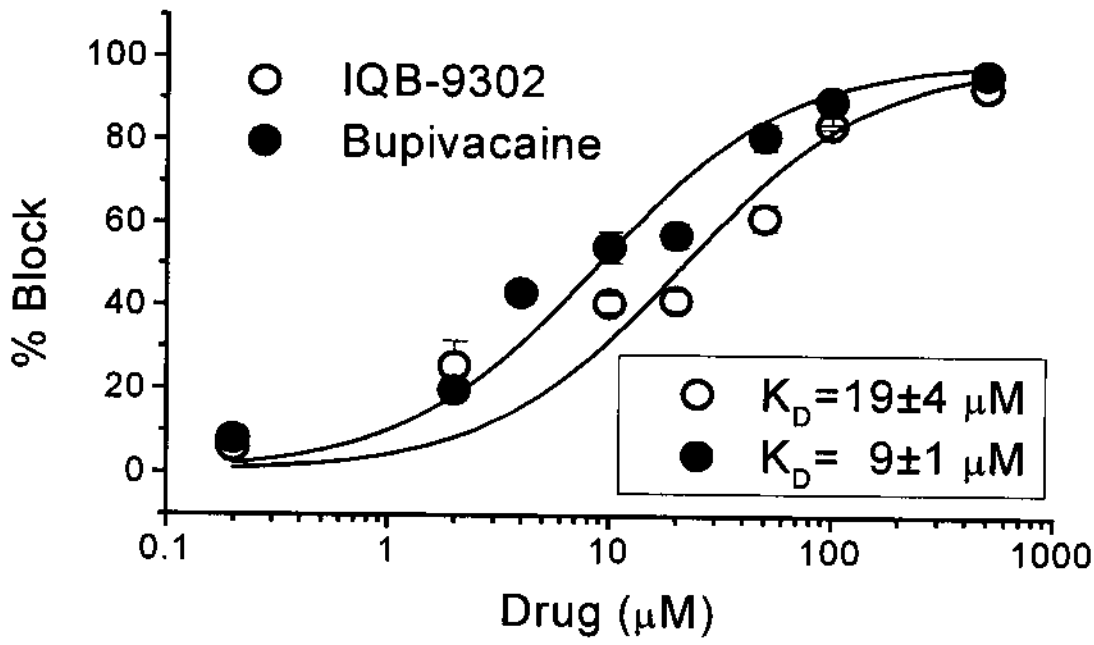
100
80
60
40
20
0
% Block
IQB-9302
Bupivacaine
K_D=19±4 μM
K_D= 9±1 μM
0.1
1
10
100
1000
Drug (μM)

Figure 7

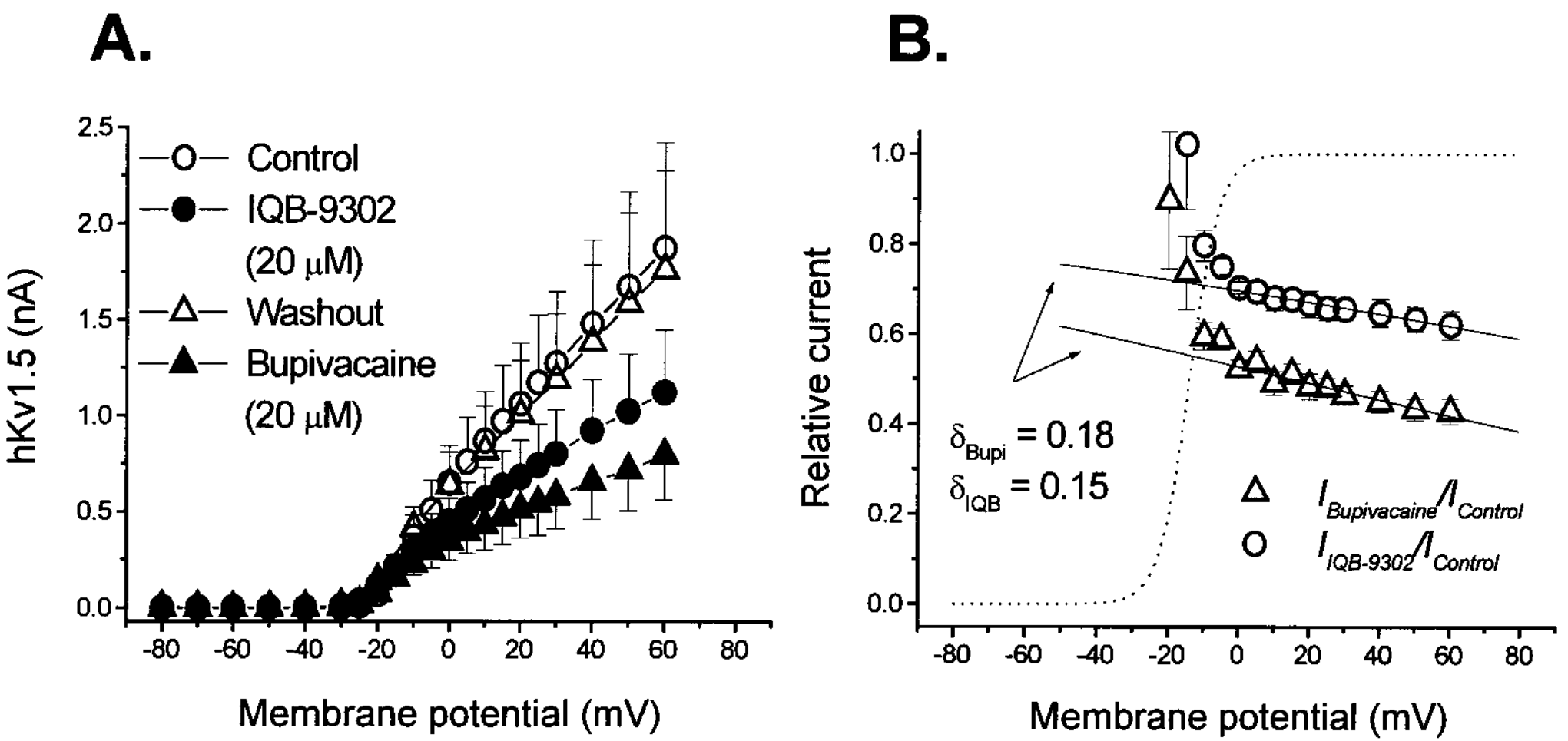
A.
B.
hKv1.5 (nA)
Control
IQB-9302
(20 μM)
Washout
Bupivacaine
(20 μM)
Membrane potential (mV)
Relative current
δBupi = 0.18
δIQB = 0.15
IBupivacaine/IControl
IIQB-9302/IControl
Membrane potential (mV)

Figure 8

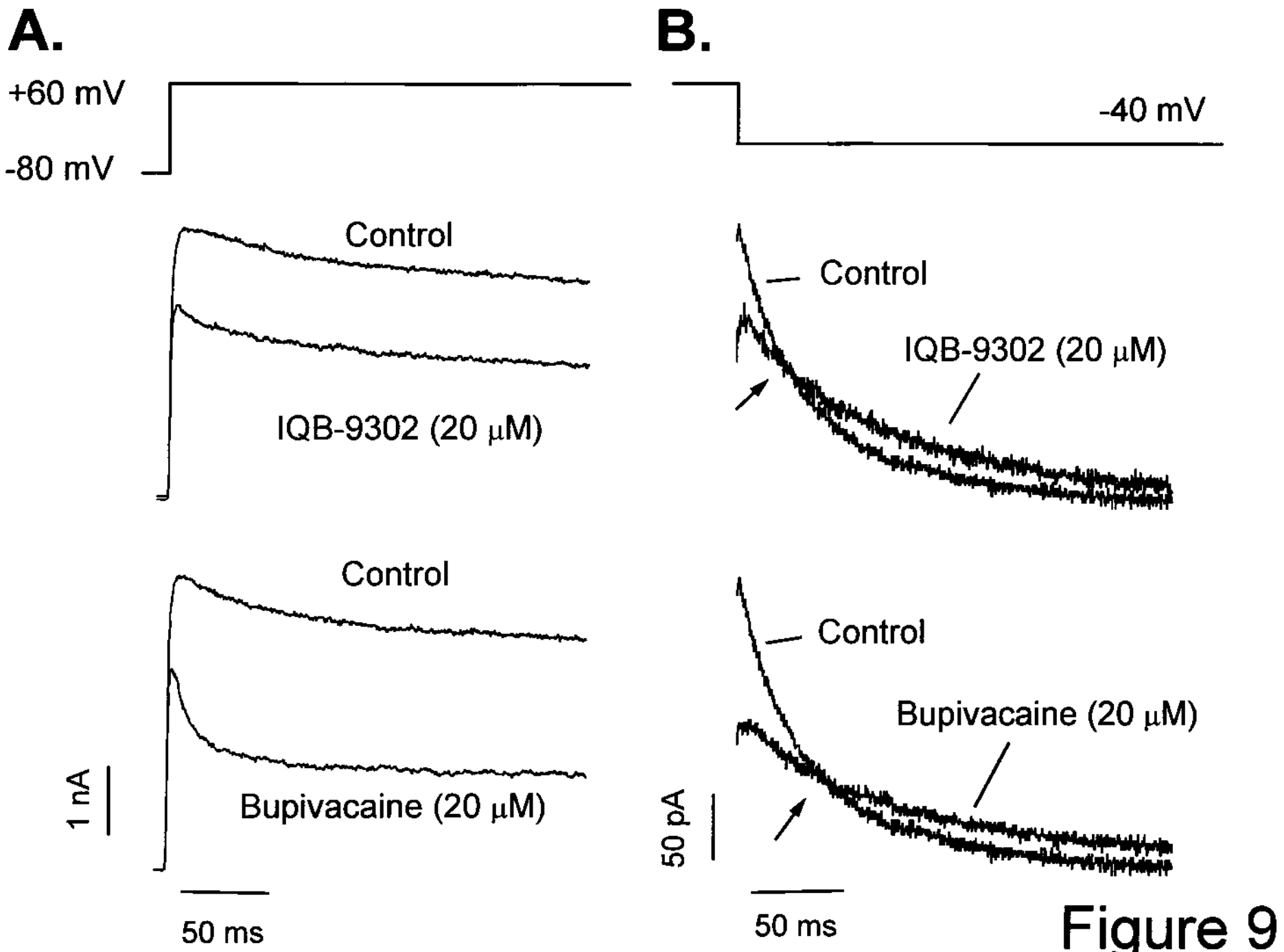
A.
+60 mV
-80 mV
Control
IQB-9302 (20 μM)
Control
Bupivacaine (20 μM)
1 nA
50 ms
B.
-40 mV
Control
IQB-9302 (20 μM)
Control
Bupivacaine (20 μM)
50 pA
50 ms

Figure 9

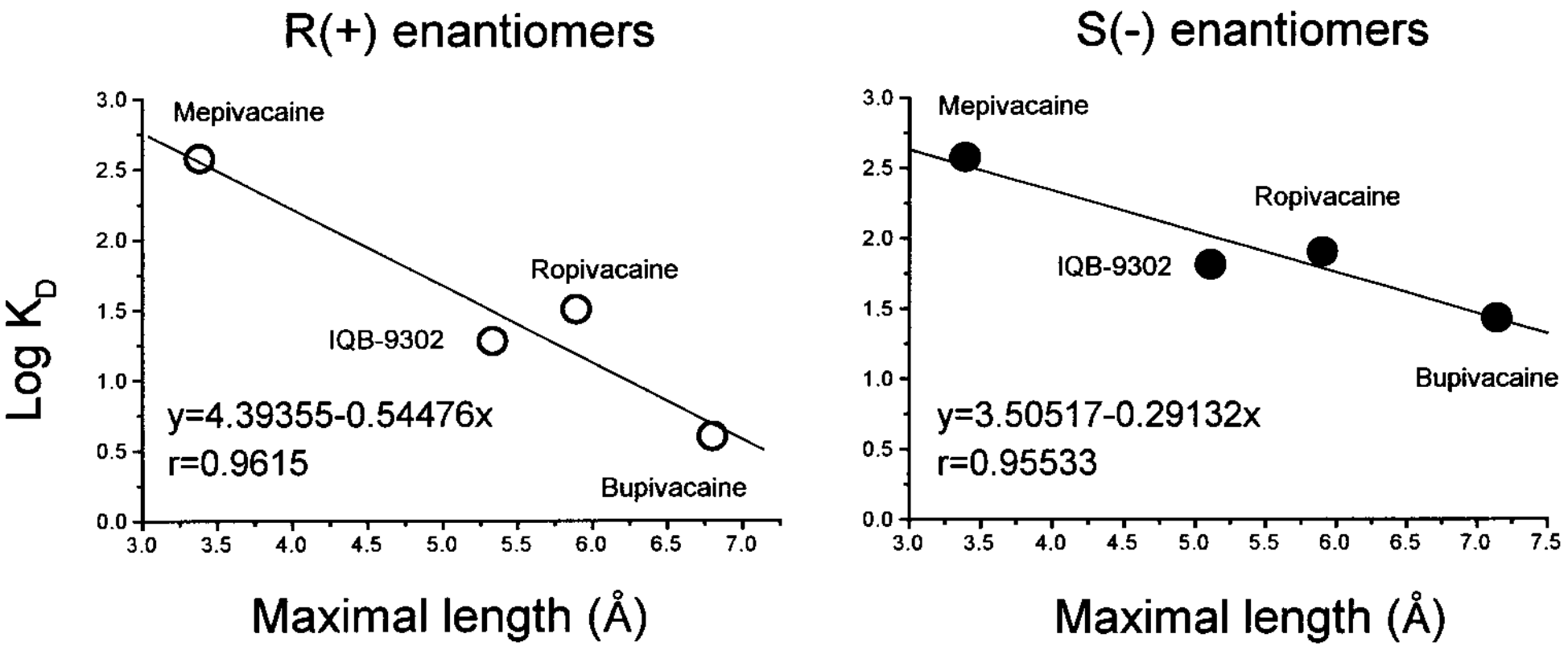
R(+) enantiomers
S(-) enantiomers
Log K_D
Mepivacaine
Ropivacaine
IQB-9302
Bupivacaine
y=4.39355-0.54476x
r=0.9615
y=3.50517-0.29132x
r=0.95533
Maximal length (Å)
Maximal length (Å)

Figure 10

A.

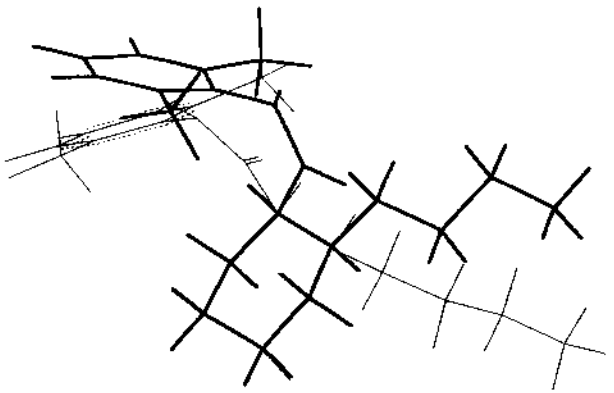

B.

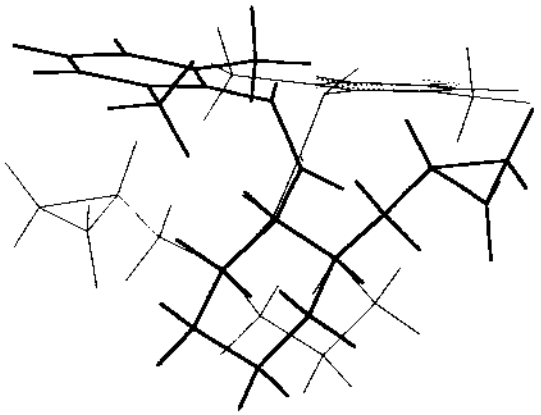

C.

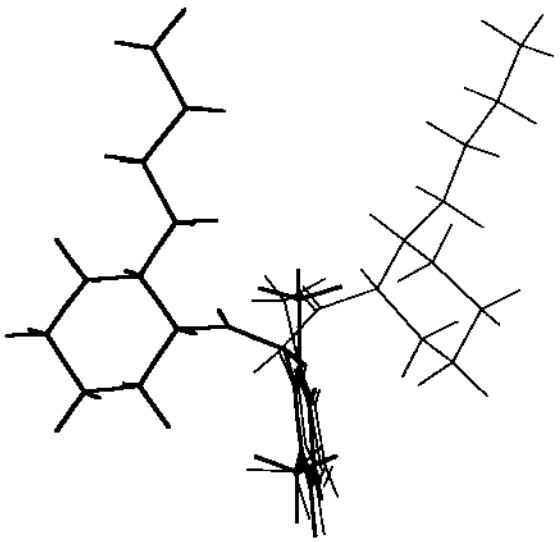

D.

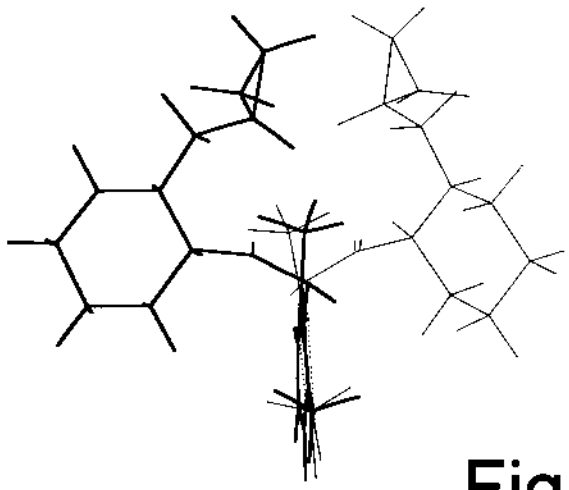

Figure 11